Influence of Concentration Fluctuations on the Dielectric α-Relaxation in Homogeneous Polymer Mixtures

G. Katana,† E. W. Fischer,* and Th. Hack

Max-Planck-Institut für Polymerforschung, Postfach 3148, 55021 Mainz, Germany

V. Abetz‡

École d'Application des Hauts Polymères, Université Louis Pasteur, 4 rue Boussingault, 67000 Strasbourg, France

F. Kremer

Fachbereich Physik, Universtät Leipzig, Linné Strasse 5, 04103 Leipzig, Germany

Received April 25, 1994; Revised Manuscript Received January 30, 1995®

ABSTRACT: The dynamics of the α-relaxation in homogeneous mixtures of polystyrene (PS) and poly(cyclohexyl acrylate-*stat*-butyl methacrylate) (P(CHA-*stat*-BMA)) is analyzed within the framework of a concentration fluctuation model. The shape and widths of the dielectric relaxation spectra as well as the range of calorimetric glass transition in the mixtures are respectively associated with distributions of relaxation time and glass transition temperature arising from the presence of concentration fluctuations. The magnitude of these fluctuations is obtained by fitting the dielectric loss curves to a model function obtained as a convolution of a relaxation time distribution for the mixture with a function describing the dielectric loss of the dielectrically active component. The relaxation time distribution is calculated from William–Landel–Ferry (WLF) or Vogel–Fulcher–Tammann (VFT) free volume scaling with the assumption of a Gaussian concentration distribution in the samples. Fits of the measured α-relaxation spectra which are dominated by P(CHA-*stat*-BMA) offer as a result the mean square concentration fluctuations $\langle(\delta\phi)^2\rangle$ in the mixtures. The fluctuations are interpreted in terms of the random phase approximation, and it is shown that $\langle(\delta\phi)^2\rangle$ is correlated to the length scale of cooperativity governing the relaxation process near the glass transition. The temperature and composition dependence of both $\langle(\delta\phi)^2\rangle$ and the size of the domains of cooperativity in PS/P(CHA-*stat*-BMA) are determined.

Introduction

The broadening of glass transition dispersions in both polymer–polymer mixtures and polymer–diluent systems constitutes a fundamental physical phenomenon which has recently become of great interest in theoretical and experimental condensed matter physics. The major problem is to obtain a physically appealing interpretation of the molecular dynamics in these systems near the glass transition temperature. As is commonly observed, macroscopic homogeneous polymer mixtures and polymer–plasticizer systems display only one calorimetric glass transition temperature intermediate within the glass transition temperature of the pure components.[1–3] The temperature range of the glass transition is however higher in the mixtures than in the pure components. This broadening is also reflected in the primary relaxation process (α-relaxation) where the relaxation spectra as revealed by different experimental techniques such as NMR,[4] dynamic mechanical spectroscopy,[5–7] light scattering,[8] and dielectric spectroscopy[9–12] are broader in the mixtures than the corresponding pure component spectra. Dynamic heterogeneities also have been observed by ESR spectroscopy.[13]

This well-known effect has until recently been qualitatively associated with the concentration fluctuations present in such systems.[14–17] Since fluctuations in composition are specific to mixtures, the broad glass transition dispersions and absorptions can be related to the free energy of mixing and its dependence on composition. This should offer a link between the observed broadening and thermodynamic variables or between dynamic and structural effects.

Recently a theoretical model based on concentration fluctuations in mixtures was proposed by Fischer et al.[18] to give a more quantitative description of the broad dispersions in the vicinity of the glass transition. This model was applied for the first time to analyze the dynamics of the α-relaxation in the mixtures PS/PVME.[18,19] A different approach based on the coupling model of relaxation[20] has been used by Roland et al.[21] to analyze segmental relaxation spectra in mixtures near the glass transition temperature. These authors also attributed the observed broadening of the glass transition dispersions in mixtures to the presence of local composition heterogeneity. As a result of their analysis, they obtained a distribution of coupling parameters of each component which measures the degree of cooperativity of segmental relaxation. The requirement that the system in question should be thermorheogically simple and therefore obeying the time–temperature superposition principle, however, restricts the application of this model to systems where these conditions are almost satisfied.

In this report we show the analysis of the influence of concentration fluctuations on the molecular dynamics in binary polymer mixtures using the concentration fluctuation model according to Fischer and Zetsche.[18] By analyzing the correlation function of the concentration fluctuations at a more coarse scale and demanding statistical independence for lattice cells, we demonstrate that a "coarse-graining" volume with a unique glass transition temperature (constant concentration fluctuation amplitude) can be defined, the size of which

† Permanent address: Department of Physics, Kenyatta University, P.O. Box 43844, Nairobi, Kenya.

‡ Permanent address: Institut für Organische Chemie, Johannes-Gutenberg-Universität Mainz, Postfach 3980, 55099 Mainz, Germany.

® Abstract published in *Advance ACS Abstracts,* March 1, 1995.

0024-9297/95/2228-2714$09.00/0

determines the extent of cooperativity in the glass transition dynamics. We apply this model to analyze the dielectric α-relaxation in mixtures of a statistical copolymer poly(cyclohexyl acrylate-*stat*-butyl methacrylate) (P(CHA-*stat*-BMA)) and polystyrene (PS). By combining the results obtained from this analysis with small-angle neutron scattering measurements on the same system, the size and the temperature dependence of the domains of cooperativity are determined.

Concentration Fluctuation Model

A striking feature of the dynamics of the dielectric α-relaxation in mixtures is its deviation from Debye-like processes and the strong temperature dependence of the shape and hence its relaxation time distribution.[9-12] This leads to a breakdown of the time–temperature superposition principle for miscible polymers in the glass transition region. Whereas the relaxation process in single-component systems can well be described by non-Debye relaxation functions, for example, the Havriliak–Negami function,[22,23] a physical interpretation of the α-relaxation in mixtures should take into account the influence of mixing on the relaxation behavior. The concentration fluctuation model describes the dynamics of the α-relaxation in mixtures by the inclusion of a relaxation time distribution which characterizes the effect of mixing on the relaxation function which is assumed to be dominated by one component. The presence of concentration fluctuations should lead to fluctuations of concentration-dependent properties of the mixture. If the variable property is a response to an external field (e.g., electric), it will show a spread corresponding to the distribution of the concentration. The mean square deviation of such a "concentration-dependent" variable $R(\phi)$ can be deduced from basic statistical mechanics[24] and is given by

$$\langle(\delta R)^2\rangle_{\langle\phi\rangle} = \left[\left(\frac{dR}{d\phi}\right)^2\right]_{\phi=\langle\phi\rangle}\langle(\delta\phi)^2\rangle \tag{1}$$

The original formulation of the concentration fluctuation model is based on the following assumptions:

The presence of local concentration fluctuations enables the sample to be divided into i subcells of size V, each of which has a concentration ϕ_i. A "coarse-graining" volume V_a is introduced, and one has to determine the size of this volume for which a unique glass transition temperature $T_g^i(\phi_i)$ can be defined for the ith subcell.

The concentration distribution $p(\phi_i)$ in the sample is Gaussian with a variance $\langle(\delta\phi)^2\rangle$.

$$p(\phi_i) \propto \exp\left[\frac{-(\phi_i - \phi_0)^2}{2\langle(\delta\phi)^2\rangle}\right] \tag{2}$$

This approximation is justified in concentrated solutions where density fluctuations are very small and the free energy of mixing (ΔF) is related to concentration fluctuations by

$$\langle(\delta\phi)^2\rangle = \frac{kT}{(\partial^2\Delta F/\partial\phi^2)_{\phi=\langle\phi\rangle}} \tag{3}$$

where $\delta\phi$ is the fluctuation in a volume element ΔV, T is temperature, and k is the Boltzmann constant.

The system is incompressible which is equivalent to the requirement that density fluctuations do not exist. Within the measurement time, the concentration fluctuations are considered to be stationary; i.e., the lifetimes of the concentration fluctuations are much longer than the relaxation time of the α-process.

The glass transition temperature of the macroscopic sample is concentration dependent and the same concentration dependence $T_g^i(\phi_i)$ is assumed to apply in every subcell.

For systems obeying the VFT equation, a relaxation time distribution of the mixture is obtained by using either the WLF or VFT equations which relate the measurement temperature with a characteristic relaxation time τ. The reference temperature is taken as the average $T_g(\phi_i)$. Thus from the WLF equation

$$\log\tau = \log\tau_g - \frac{C_1(T - T_g)}{C_2 + (T - T_g)} \tag{4}$$

a relaxation time $\tau_i(\phi_i,T)$ can be defined for each subcell i. For a given temperature T,

$$\langle(\delta\log(\tau/\tau_g))^2\rangle = \left(\frac{d\log(\tau/\tau_g)}{dT_g}\right)^2_{T_g=\langle T_g\rangle}\langle(\delta T_g)^2\rangle = \left\{\frac{C_1C_2}{(C_2 + T - T_g)^2}\right\}^2_{T_g=\langle T_g\rangle}\langle(\delta T_g)^2\rangle \tag{5}$$

From the concentration dependence of the glass transition temperature, eq 5 can be expressed as

$$\langle(\delta\log(\tau/\tau_g))^2\rangle = \left(\frac{d\log(\tau/\tau_g)}{dT_g}\right)^2_{T_g=\langle T_g\rangle}\left(\frac{dT_g}{d\phi_B}\right)^2_{\phi=\langle\phi_B\rangle}\langle(\delta\phi)^2\rangle \tag{6}$$

where the first term on the right-hand side gives the temperature dependence and the product of the second and third terms the concentration dependence. Although the fluctuations in T_g are directly dependent on the concentration fluctuations, the fluctuations in temperature during measurement are statistically independent of the concentration fluctuations,[24] i.e., $\langle\delta T\delta\phi\rangle = 0$ and

$$\langle(\delta\log(\tau/\tau_g))^2\rangle = \frac{\partial^2\delta\log(\tau/\tau_g)}{\partial T^2}\langle(\delta T)^2\rangle + \frac{\partial^2\delta\log(\tau/\tau_g)}{\partial\phi^2}\langle(\delta\phi)^2\rangle \tag{7}$$

The influence of the temperature fluctuations on the relaxation time distribution can be neglected since dielectric measurements are usually performed at quasi-thermal equilibrium conditions.

Dielectric α-Relaxation Function for a Mixture. This is evaluated for a mixture in which the relaxation behavior is dominated by one component. It is assumed that within each subvolume the shape of the dielectric function $\epsilon^*_A(\omega)$ for the polar component is the same as that in the pure state and can be described by a relaxation function, in the case of P(CHA-*stat*-BMA), the Havriliak–Negami function with the shape parameters α and γ

$$\epsilon^*_A(\omega) = \epsilon'(\omega) - i\epsilon''(\omega) = \epsilon_\infty + \frac{\epsilon_s - \epsilon_\infty}{(1 + (i\omega\tau)^\alpha)^\gamma} \tag{8}$$

with $0 < (\alpha,\gamma) \leq 1$. α and γ are dimensionless param-

eters describing the symmetric and asymmetric broadening of the loss function, respectively, τ is the relaxation time scale for this function, and ϵ_s and ϵ_∞ are the low- and high-frequency values of the real part of the complex dielectric function with $\omega\tau \ll 1$ and $\omega\tau \gg 1$. $\epsilon_s - \epsilon_\infty = \Delta\epsilon$ is the dielectric relaxation strength of the process under investigation. The dielectric loss $\epsilon''_M(\omega)$ of the mixture results from the summation over all subvolumes:

$$\epsilon''_M(\omega) = \sum_i \epsilon''_i(\omega\tau_i) = \int_0^\infty n_v(\tau)\, \epsilon''_A(\omega\tau)\, d\tau \qquad (9)$$

with $\epsilon''_A(\omega\tau)$ being the imaginary part of the Havriliak–Negami function of the polar component (eq 8) determined at the same temperature interval $T - T_g(\phi_i)$ in the mixtures. The distribution of relaxation time $n_v(\tau)$ is obtained by first transforming the concentration distribution into a distribution of glass transition temperatures $n_v(T_g)$ by using the macroscopic concentration dependence of the glass transition temperatures for a given homogeneous polymer mixture. $n_v(T_g)$ is related to the concentration distribution (eq 2) as

$$n_v(T_g) \propto \frac{1 - \phi(T_g)}{1 - \phi_0} \frac{1}{\sqrt{2\pi\langle(\delta\phi)^2\rangle}} \exp\left(\frac{-(\phi(T_g) - \phi_0)^2}{2\langle(\delta\phi)^2\rangle}\right) \qquad (10)$$

where $\phi(T_g)$ is obtained from the inversion of the macroscopic relation giving the concentration dependence of the glass transition temperature in the mixture. The prefactor $[1 - \phi(T_g)]/(1 - \phi_0)$ weights each subvolume with the content of the component that dominates the relaxation function. Secondly, the WLF equation (eq 4) is inverted to

$$[T - T_g](\tau) = \frac{-C_2 \log(\tau/\tau_g)}{C_1 + \log(\tau/\tau_g)} \qquad (11)$$

which gives the temperature shift factor $[T - T_g]$ for a given change of the logarithm of the relaxation time log τ – log τ_g. Inserting eq 11 in $\phi(T_g)$ leads to $\phi(\tau,T)$, which can be substituted into eq 2 to provide a distribution of relaxation time in terms of $\langle(\delta\phi)^2\rangle$.

Transformation of eq 9 on the logarithmic scale yields a convolution product $L(x) \otimes \epsilon''(-x)$:

$$\epsilon''_M(\log\omega) = \int_{-\infty}^{\infty} L(\log\tau)\, \epsilon''_A(\log\omega + \log\tau)\, d\log\tau \qquad (12)$$

with $L(\log\tau) = \tau n_v(\tau)$. The experimental data can be fitted to this function with $\langle(\delta\phi)^2\rangle$ contained in $n_v(\tau)$ used as the only fit parameter. As mentioned before, we will apply this model to analyze the dielectric α-relaxation process in a new system PS/P(CHA-*stat*-BMA), which like PS/PVME exhibits a lower critical solution temperature (LCST).

Experimental Section

Sample Preparation and Characterization. The acrylate polymers used were a statistical copolymer, poly(cyclohexyl acylate-*stat*-butyl methacrylate) (P(CHA-*stat*-BMA)) provided by Röhm AG, Darmstadt, and polystyrene obtained from Polymer Standard Service, Mainz. For small-angle neutron scattering (SANS) studies, a deuterated polystyrene (PSD) was used instead of the protonated one. For comparison, also one deuterated blend was investigated by dielectric spectroscopy, and no influence of the substitution on the dielectric loss behavior was found. The composition of the copolymer was determined by using ^{1}H-NMR spectroscopy. Table 1 shows the chemical structure and properties of the polymers used in the study. Mixtures PS/P(CHA-*stat*-BMA) of varying composition were prepared by dissolving the desired amounts of the polymers at a 10% level (g/mL) of the total polymer in tetrahydrofuran (THF). Films for the mixtures as well as for the pure components were solution cast using the same solvent. For non-self-supporting films, the solution was poured directly on a gold-plated steel electrode which was held tightly in a specially prepared Teflon ring. The electrodes were covered with aluminum cups to minimize the rate of solvent evaporation. In the case where samples phase separated when dried at room temperature, the solutions were placed in a desiccator with silica gel and freeze-dried. After the solvent was evaporated, the films were first air-dried for 2 days at 296 K and then for a further 5 days under vacuum using a selected drying program which raised the temperature at 1 K steps per hour until the sample acquired a temperature T_g + 20 K. The sample was then cooled at the same rate to room temperature. The resulting films for the dielectric measurements were 0.2 ± 0.01 mm thick. Extra thin films (100 μm) were prepared in Petri dishes for the determination of the cloud point temperature. The glass transition temperatures of the mixtures and the mixture components were determined using a Mettler DSC30 at scanning rate of 10 K/min. Several runs were made to ensure a uniform thermal history. This was done until reproducible scans were obtained, and all glass transition temperatures T_g were taken as the temperature corresponding to half of the heat capacity change. Cloud points were determined by light scattering at different heating rates. The cloud point temperature T_c was obtained by extrapolating to a heating rate equal to zero. Figure 1 shows the cloud point and the glass transition temperatures as a function of PS composition. The composition dependence of the glass transition temperature for this system is well described by the Fox equation for mixtures (solid line)

Table 1. Chemical Structures and Properties of the Pure Polymers

Structures and Abbreviations	M_w [g/mol]	M_w/M_n	T_g [K]
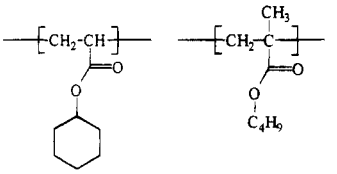 CHA (39 mol%) BMA (61mol %)	415000	1.88	291
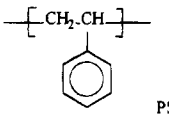 PS	198000	1.04	379
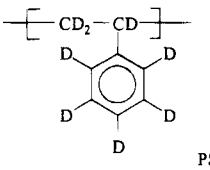 PSD	99000	1.07	379

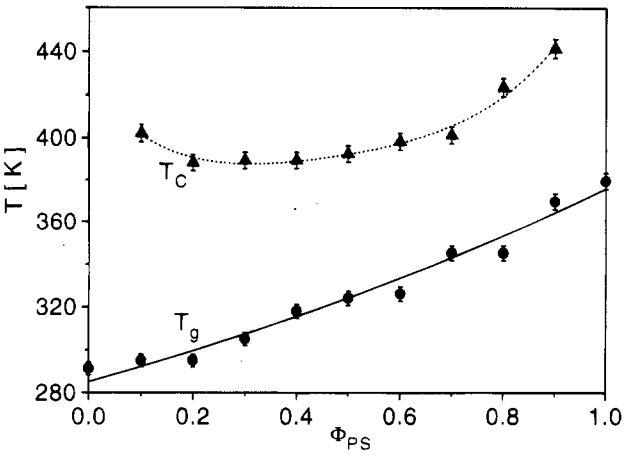

Figure 1. Phase diagram and concentration dependence of the glass transition temperature for mixtures PS/P(CHA-*stat*-BMA). (▲) are the cloud temperatures T_c measured by light scattering and (●) are the calorimetric glass transition temperatures T_g. The composition dependence of T_g is well described by the Fox equation (eq 13).

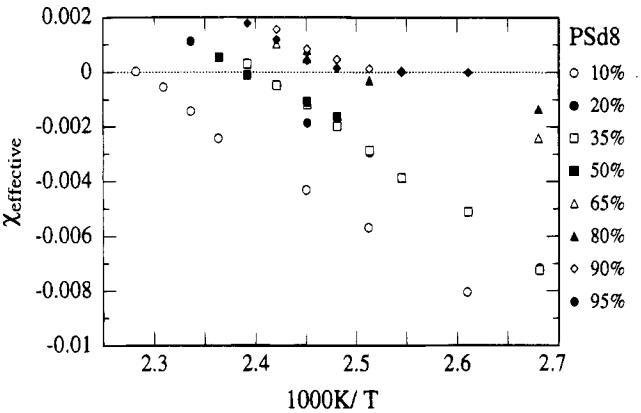

Figure 2. Composition and temperature dependence of the effective interaction parameter χ_{eff} in the mixtures PSD/P(CHA-*stat*-BMA) determined by small-angle neutron scattering (SANS). Reference volume is the PSD repeating unit.

$$\frac{1}{T_g} = \frac{w_1}{T_{g_1}} + \frac{w_2}{T_{g_2}} \tag{13}$$

where w_1 and w_2 are the respective weight fractions of the first and second components, T_{g_1} and T_{g_2} are their glass transition temperatures, and T_g is the glass transition temperature of the mixture. The densities of the pure components and their mixtures were determined by using a density gradient column composed of 2-propanol, distilled water, and calcium nitrate at 296 K. The effective interaction parameter χ_{eff} as determined by small-angle neutron scattering measurements (SANS)[25,26] for mixtures of PSD/P(CHA-*stat*-BMA) is shown in Figure 2.

Dielectric Measurements. Dielectric measurements were performed on the polymers and their blends with a PS composition by weight varying from 10 to 80%. Self-supporting gold-plated films were placed between two gold-plated stainless steel electrodes that were pressed together by a micrometer screw. The effective diameter of the samples was 20 mm and their thickness was 0.2 ± 0.01 mm. Measurements of the complex dielectric function were made in the frequency range 10^{-1}–10^{6} Hz using a frequency response analyzer (Solartron–Schlumberger FRA 1260 with a high-impedance preamplifier of variable gain) and a Hewlett-Packard impedance analyzer (HP4192A, frequency range from 10 to 10^7 Hz).[18] The highest temperature of measurement in the one-phase region for the mixtures was about 10 K below the cloud point curve. Below 450 K the temperature was controlled by a nitrogen gas heating system which covers a range from 90 to 450 K with a temperature stability within ±0.2 K. The gas was produced by mounting a heater in a liquid nitrogen container. For higher temperatures, the same system was used with either piped nitrogen gas or air. The resulting spectra measured at different temperatures and for various compositions were fitted with the Havriliak–Negami function and the parameters α, γ, τ, and Δε were obtained. At frequencies below 10^3 Hz a conductivity contribution ϵ''_{dc} adds up to the measured dielectric loss. It obeys the power law

$$\epsilon''_{dc} = \frac{\sigma_{dc}}{\epsilon_0 \omega^s} \tag{14}$$

with $0.5 \le s \le 1$. ϵ_0 is the permittivity of vacuum, and σ_{dc} is the direct current conductivity. Since the relaxation process and the conductivity contribution strongly differ in their functional form, the two can easily be separated. The copolymer P(CHA-*stat*-BMA) has a high-frequency β-relaxation which is much weaker than the α-relaxation.[12] A twofold Havriliak–Negami function was fitted to the experimental data as shown for the pure copolymer in Figure 3 (top), and both the conductivity contribution and the high-frequency β-relaxation were subtracted. The half-widths of the α-relaxation curves were determined from the parameters α, γ, τ, and Δε obtained from the fits.

Results and Discussion

Figure 3 (bottom) shows the plot of the dielectric loss ε″ against the logarithm of frequency for the α-process in the copolymer P(CHA-*stat*-BMA) and for mixtures with composition $\phi_{PS} = 0.3$ and 0.5 with the fits using the Havriliak–Negami function (eq 8). The shape of the loss curves for P(CHA-*stat*-BMA) which are characterized by the Havriliak–Negami shape parameters α and γ (Figure 4a) is almost temperature independent. The relaxation spectra in the mixtures are much broader than those of the pure copolymer. A comparison of the shape parameters for various mixtures at the same temperature interval $T - T_g$ shows a strong composition dependence of the symmetric broadening or of the low-frequency slope when the log $\epsilon''(\omega)$ is plotted against log ω (Figure 4b). Figure 5 shows the calorimetric glass transition widths in the mixtures normalized for the differences in the glass transition temperature of the pure components plotted as a function of composition. The normalization of the observed glass transition width Γ was done using an expression proposed by Pomposo et al.[27]

$$W_c = \Delta\Gamma/\Delta\Gamma_{max} \tag{15}$$

where W_c is the corrected width, ΔΓ is the difference between the experimental width and the width of the additive component, and $\Delta\Gamma_{max}$ represents the potential width minus the additive breadth. The potential width is the difference between the end point of the transition region for the higher T_g component and the onset temperature for the lower T_g component. The temperature range of the glass transition was determined from the DSC curve as shown in the insert in Figure 5. The corrected widths indicate a broadening of the glass transition in mixtures with a maximum broadening occurring between $\phi_{PS} = 0.3$ and 0.4. This observation is consistent with the braodening of the α-relaxation process in PS/P(CHA-*stat*-BMA) as has been shown in other systems.[10,17,19] By inspection, one notices that the corrected widths W_c (Figure 5) are very much less than 1. This implies that very small concentration fluctuations will be present in these mixtures. The glass transition width analysis, however, gives only a qualita-

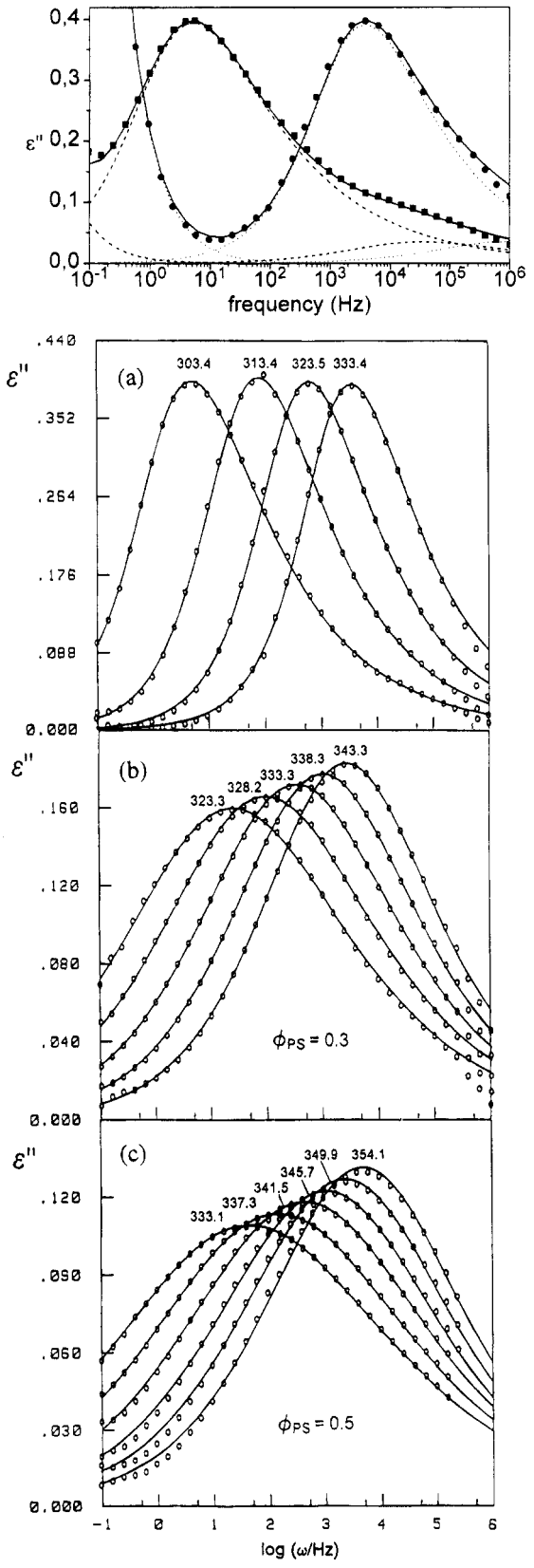

Figure 3. (Top) Dielectric loss curves $\epsilon''(\omega)$ of pure P(CHA-*stat*-BMA) for 303 (■) and 333 K (●). Contributions from dc conductivity, α-relaxation, and β-relaxation are indicated by dashed lines for 303 K and dotted lines for 333 K. Superpositions of the different contributions are given by solid lines. (Bottom) Comparison of the dielectric loss curves $\epsilon''(\omega)$ in pure P(CHA-*stat*-BMA) (a) and in mixtures with ϕ_{PS} = 0.3 (b) and 0.5 (c). The fits were performed using the Havriliak–Negami function (eq 8). β-relaxation and dc conductivity have been subtracted.

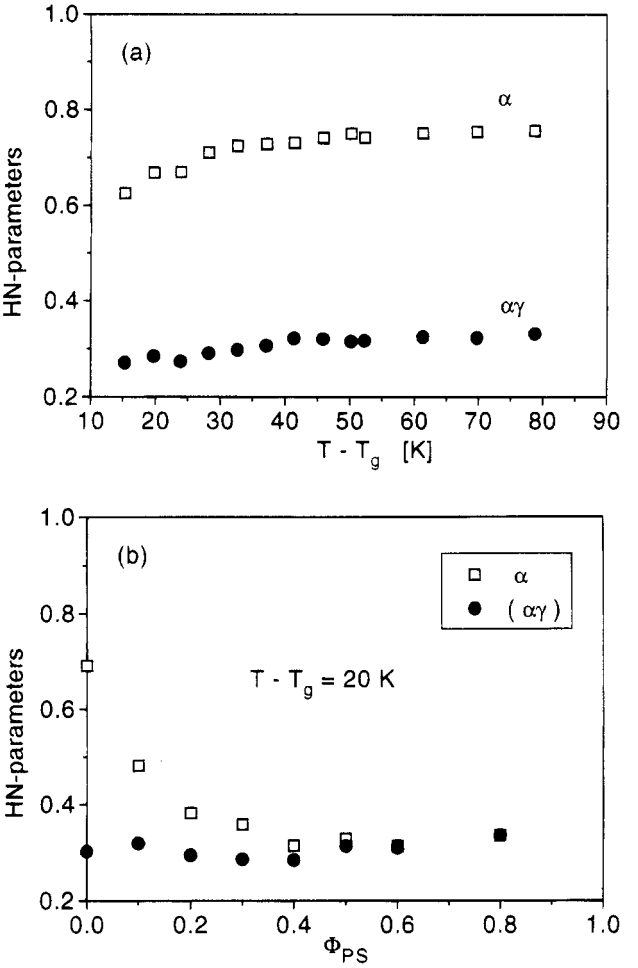

Figure 4. Havriliak–Negami shape parameters α and αγ plotted against $T - T_g$ for the polar P(CHA-*stat*-BMA) (a) and $\alpha(\phi_{PS})$ and $\alpha\gamma(\phi_{PS})$ taken at $T - T_g = 20$ K plotted as a function of composition (b).

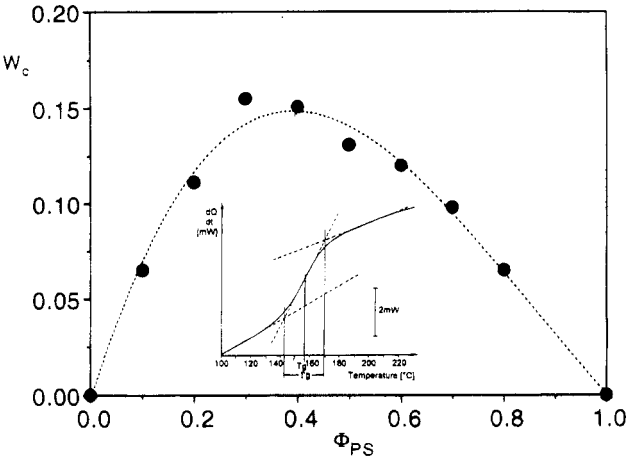

Figure 5. Normalized width of the calorimetric glass transition region as a function of composition for PS/P(CHA-*stat*-BMA) mixtures. The insert shows how the temperature range of the glass transition was determined from DSC thermograms.

tive picture of the extent of the influence of the concentration fluctuations on the glass transition dispersions.

The concentration fluctuation model associates the broadening effect with concentration fluctuations present in the mixtures. A relaxation function describing the relaxation process in the mixture is obtained by making a Gaussian approximation of the concentration fluctua-

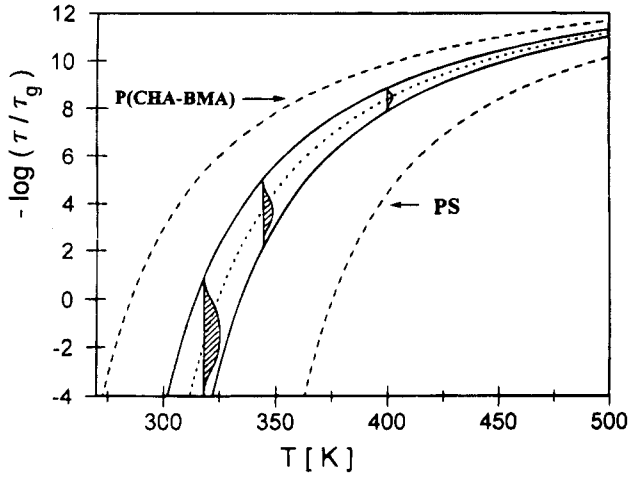

Figure 6. WLF behavior for the pure components PS and P(CHA-*stat*-BMA) and a 50/50 mixture. The temperature dependence of the width of the time distribution is shown for a constant concentration fluctuation $|\delta\phi| = 0.01$.

tions and assuming that the function is dominated by one component only.[18] A comparison of the loss curves in Figure 3 shows that at a given temperature the curves in the mixtures are shifted in their frequency positions relative to those of the pure P(CHA-*stat*-BMA). Figure 6 shows the temperature dependence of the relaxation time for PS and P(CHA-*stat*-BMA) and for a 50/50 mixture. All systems exhibit a Vogel–Fulcher–Tamann free volume scaling of the temperature dependence of the relaxation time, enabling the evaluation of relaxation time distributions for the mixtures. Figure 7a shows distributions of T_g in various mixtures evaluated from the concentration dependence given by eq 13. The distribution of relaxation times in a mixture with a mean concentration $\phi_{PS} = 0.5$ at various temperature intervals $T - T_g$ is shown in Figure 7b. In the temperature range closer to T_g, the distribution is much broader and becomes narrower as $T - T_g$ increases. It is apparent from eqs 4 and 5 that if $dT_g/d\phi \approx$ constant, then for very large intervals $(T - T_g)$, $d \log(\tau/\tau_g)/dT_g \rightarrow 0$, and for a given $\langle(\delta T_g)^2\rangle$ which is associated with the variance of the concentration distribution (eq 6), the distribution of relaxation time becomes narrower at higher temperatures, almost acquiring a constant value as illustrated in Figure 6.

Comparing the temperature dependencies of the half-widths of the calculated relaxation time distributions and the half-widths of the experimentally determined frequency distributions (Figure 8), the following features are observed. First, the half-widths of the frequency distribution $\delta_{1/2} \log \omega$ show the scaling law $(\delta_{1/2} \log \omega)^{-1} \propto T - T_g$ while the half-widths of the relaxation time distributions $\delta_{1/2} \log(\tau/\tau_g)$ scale with temperature as $(\delta_{1/2} \log(\tau/\tau_g))^{-1/2} \propto T - T_g$. The temperature dependence of the half-widths of the relaxation time distribution conforms with the predictions of eq 6 if $d\tau_g/d\phi_{PS} \approx$ constant and for a constant $\langle(\delta\phi)^2\rangle$ and can easily be deduced from the VFT equation. By using the WLF or the VFT scaling, it has been shown by Donth[28] that the broadening of a spectrum $\delta_{1/2} \log \omega$ is related to the Vogel temperature T_0 by $(\delta_{1/2} \log \omega)^{-1} \propto T - T_0$, which is in good agreement with our results. It is notable (Figure 8) that the half-widths of both the time and the frequency distributions diverge at $|T - T_g| \approx C_2$, the second WLF parameter which corresponds to a temperature $T = T_0$.

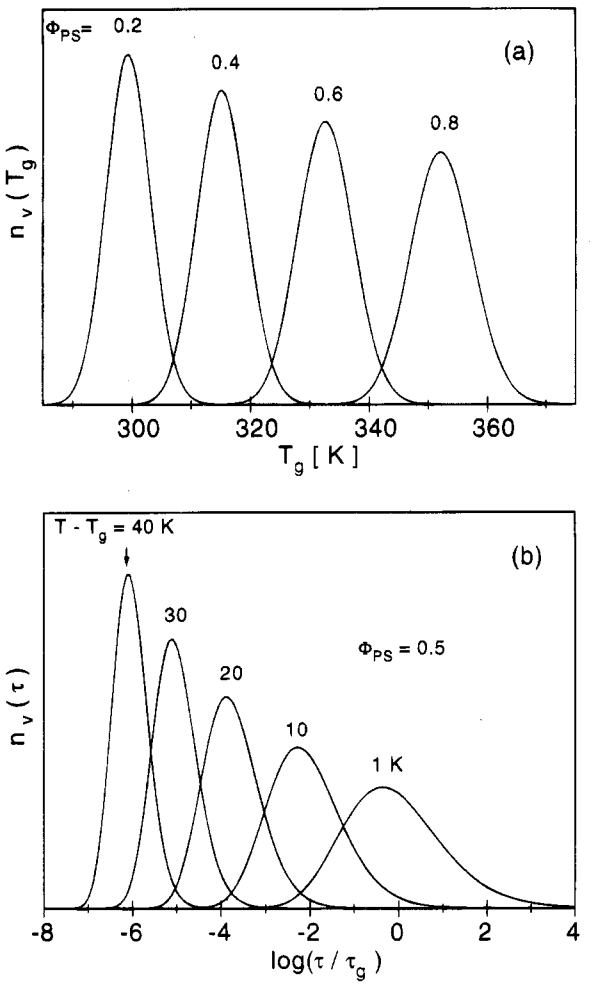

Figure 7. Distributions of (a) glass transition temperature calculated for various PS/P(CHA-*stat*-BMA) mixtures with a constant concentration fluctuation $|\delta\phi| = 0.05$ and (b) relaxation times for a mixture with a mean concentration $\phi_{PS} = 0.5$ evaluated at various temperature intervals $T - T_g$.

Table 2. Mean Square Concentration Fluctuation Values at Different Temperatures Obtained from the Analysis of the Dielectric Loss Curves for Various Mixtures Using the Concentration Fluctuation Model

$\phi_{PS} = 0.2$		$\phi_{PS} = 0.3$		$\phi_{PS} = 0.4$		$\phi_{PS} = 0.5$	
T (K)	$\langle(\delta_\phi)^2\rangle$	T (K)	$\langle(\delta\phi)^2\rangle$	T (K)	$\langle(\delta\phi)^2\rangle$	T (K)	$\langle(\delta\phi)^2\rangle$
319.6	0.0037	318.3	0.0025	328.1		328.9	0.0022
323.9	0.0042	323.3	0.0030	333.1	0.0030	333.1	0.0025
328.1	0.0046	328.2	0.0036	336.3	0.0035	337.3	0.0029
332.4	0.0051	333.3	0.0041	341.5	0.0040	341.5	0.0032
336.6	0.0054	338.3	0.0046	345.7	0.0046	345.7	0.0035
340.9	0.0060	343.3	0.0051	349.9	0.0051	349.9	0.0038
345.2	0.0062	348.2	0.0056	354.1	0.0054	354.1	0.0041
349.5	0.0062	353.3	0.0060	357.9	0.0060	357.9	0.0045
353.0	0.0073			361.9	0.0062	361.9	0.0045

Figure 9 shows the experimental dielectric loss spectra for various mixtures fitted to eq 12 with $\langle(\delta\phi)^2\rangle$ as a fit parameter. The relaxation function maps the experimental curves very well. The mean square concentration fluctuations obtained from the fits are plotted as a function of $T - T_g$ (Figure 10). Table 2 shows the values of $\langle(\delta\phi)^2\rangle$ obtained for various mixtures at the temperatures corresponding to the temperature of measurement of the dielectric loss curves. It is noteworthy that the variance of the concentration distribution plotted against $T - T_g$ is composition independent in the composition range $\phi_{PS} = 0.2$–0.5. This observation conforms well with the fact that the half-widths of the

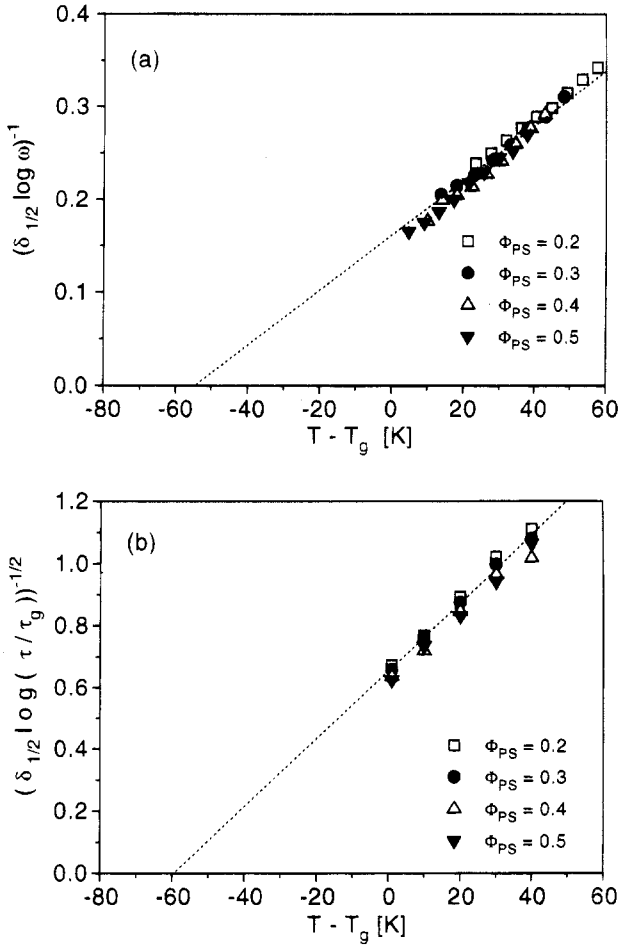

Figure 8. Comparison of the temperature dependence of the half-widths of the frequency (a) and relaxation time (b) distributions of various mixtures.

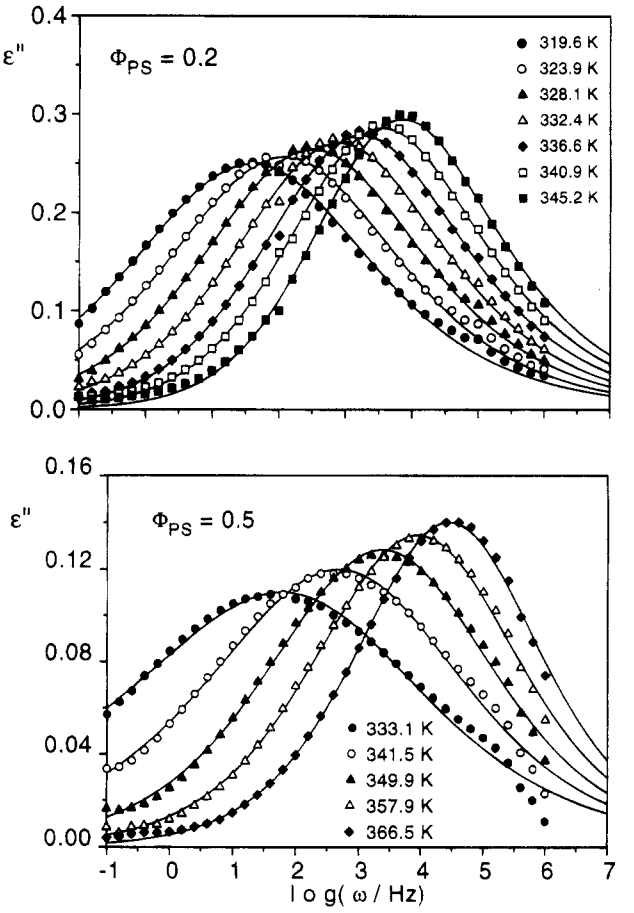

Figure 9. Measured dielectric loss curves for the mixtures PS/P(CHA-*stat*-BMA) with $\phi_{PS} = 0.2$ and 0.5, fitted with eq 12 of the concentration fluctuation model with $\langle(\delta\phi)^2\rangle$ used as a fit parameter.

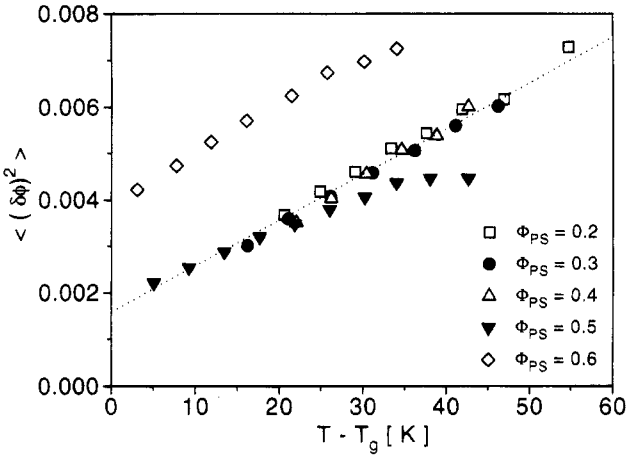

Figure 10. Mean square concentration fluctuations $\langle(\delta\phi)^2\rangle$ as a function of $T - T_g(\phi_{PS})$. The composition dependence of $\langle(\delta\phi)^2\rangle$ reflects the composition dependence of the half-widths of both the frequency and time distributions shown in Figure 8.

experimentally determined frequency distributions plotted as a function of $T - T_g$ (Figure 8a) showed no composition dependence. This is also true for the half-widths of the relaxation time distribution calculated for a constant $\langle(\delta\phi)^2\rangle$. The concentration and temperature dependence of the concentration fluctuations in the miscibility range is determined by the static structure factor $S(q=0)$, which also yields the concentration dependence of the interaction parameter $\chi(T)$.[25] It is remarkable that small-angle neutron scattering measurements on PSD/P(CHA-*stat*-BMA) reveal a negligible concentration dependence of $\chi(T)$ in the same composition range (Figure 2). A closer inspection of the temperature dependence of the correlation function of the concentration fluctuations (Figure 10) shows that $\langle(\delta\phi)^2\rangle$ goes to zero at $T - T_g \approx -15$ K. This temperature lies far above the ideal glass transition temperature at which the widths of the frequency and time distribution diverge. The temperature range in which the α-relaxation in miscible blends is measured lies in the region where the VFT scaling ($T < T_A$) is obeyed, with T_A being a crossover temperature which marks the transition from VFT to an Arrhenius behavior.[30] This crossover temperature in polymers does not show up within the experimentally accessible temperature window and its observation in mixtures is further limited by the position of the cloud point curve (Figure 1). The relaxation process in the VFT range $T \ll T_A$ is governed by cooperative dynamics which involve simultaneous and correlated changes of degrees of freedom of many segments in an extended region as opposed to independent motion of individual units typical in the Arrhenius range.[30] The assumption of cooperative dynamics implies the existence of "cooperatively rearranging domains" (CRD) with a characteristic lifetime of the order of the relaxation time τ_α of the α-relaxation. In mixtures it is expected that the size of the domains will be influenced by composition, especially when the components strongly vary in structure. This is in line with the observation by Ngai that the degree of intermolecular coupling associated with the relaxation of a given

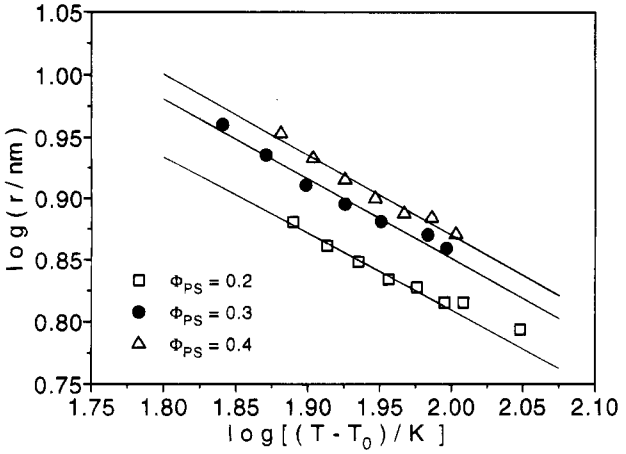

Figure 11. Size of cooperatively relaxing domains as deduced from the measured values of $\langle(\delta\phi)^2\rangle$. r scales with temperature as $r \propto (T - T_0)^{-\nu}$ with $0.60 \leq \nu \leq 0.67$. T_0 is the Vogel temperature.

segment will vary according to the composition of the local environment.[31] The freezing of the concentration fluctuations at $T - T_g = -15$ K reflects the point when their influence as seen in relation to the length scale of cooperativity becomes minimal as T_0 is approached. In the temperature range $-15 > T - T_g \geq -C_2$, density fluctuations with long wavelength dominate the relaxation behavior.

The concentration fluctuation model enables the experimental determination of the size of the domains of cooperativity[18,19] in mixtures. The Gaussian approximation of the concentration fluctuations can be utilized to relate the variance of the concentration distribution to $S(q)$ and to the form factor $F(qr)$ of a scattering volume. This is achieved analogous to the relation developed for density fluctuations by Ruland.[32] The length scale of cooperative dynamics within the glass transition is estimated by using the relation

$$\langle(\delta\phi)^2\rangle = \frac{1}{2\pi^2 r^2}\frac{a^3}{\int_0^\infty S(q)\left(\frac{3[\sin(qr) - qr\cos(qr)]}{(qr)^2}\right)^2 dq} \tag{16}$$

where $S(q)$ is the RPA structure factor and a is the average segment length. In our analysis the scattering volume is identified with a "coarse-graining volume" V_a at the minimum resolution which is characterized by a unique glass transition temperature T_g. Figure 11 shows the temperature dependence of the radius of a spherical domain of cooperativity in various mixtures. The mean domain radius r increases as the temperature decreases, in agreement with various theoretical predictions.[32-34] The radius obeys the scaling law $r \propto (T - T_0)^{-\nu}$, where values of ν between 0.64 and 0.67 were obtained. A similar scaling law was obtained for the length scale of the glass transition in *o*-terphenyl determined by combining depolarized dynamic light scattering, photon correlation spectroscopy, and viscosity experiments.[34] In the treatment of Adam and Gibbs,[33] it was assumed that the apparent activation energy is proportional to the size of the unit that must move cooperatively. A similar assumption was made by Matsuoka.[35] Figure 12 shows a double-logarithmic plot of the variation of the apparent activation energy E_a with temperature obtained from the WLF relation

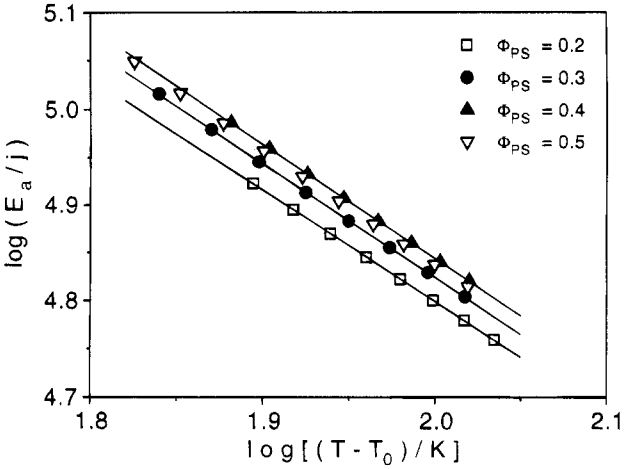

Figure 12. $\log(E_a)$ vs $\log(T - T_0)$ evaluated from eq 14. The WLF parameters used are those of the P(CHA-*stat*-BMA), which is assumed to dominate the relaxation process in the mixtures. $E_a \propto (T - T_0)^{-1}$.

Table 3. Scale of Cooperativity r at T_g Estimated from DSC Thermograms Using Equation 15 and Values Obtained from the Concentration Fluctuation Model

mixture with PS conc Φ_{PS}	$r \pm 0.5$ (nm) (DSC)	$r \pm 1$ (nm) (CFM)
P(CHA-*stat*-BMA)	2.4	3.7
0.2	3.6	6.3
0.3	4.3	7.0
0.4	5.2	7.5
0.5	5.5	7.5
0.6	7.0	
0.7	9.0	
PS	4.5	

$$E_a = \frac{RT^2C_1C_2}{[C_2 + (T - T_0)]^2} \tag{17}$$

where the WLF parameters are assumed to be equal to those of the polar component. R is the gas constant, and the Vogel temperature $T_0(\phi)$ is also composition dependent. The apparent activation energy evaluated for the α-relaxation in the mixtures varies inversely proportionally with $T - T_0$, leading to the relation between the activation energy and the volume of cooperativity, $E_a \propto V_a^{1/2}$. This follows from Figure 11, which shows that $V_a \propto (T - T_0)^{-2}$.

The scale of cooperativity at T_g can also be estimated from DSC thermograms by using the Donth fluctuation formula

$$V_a = \frac{kT_g^2\Delta C_p^{-1}}{\varrho(\delta T)^2} \tag{18}$$

where ϱ is the density of the bulk material, $(\Delta C_p)^{-1}$ is the relaxation strength of the reciprocal specific heat at constant pressure, and δT is the half-width of the glass transition range $\Gamma T_g/2$. Table 3 shows the values of r calculated for the homopolymers and the mixtures from DSC. For comparison some values of the length scale of cooperativity estimated from the dielectric measurements are also shown. The values of r obtained from both methods are composition dependent, with those from DSC being smaller than those obtained using the concentration fluctuation model. This difference can be accounted for by the fact that different thermodynamic activities are sensitive to different length scales.

The assumption that the temperature dependence of the relaxation time in the mixtures is the same as in

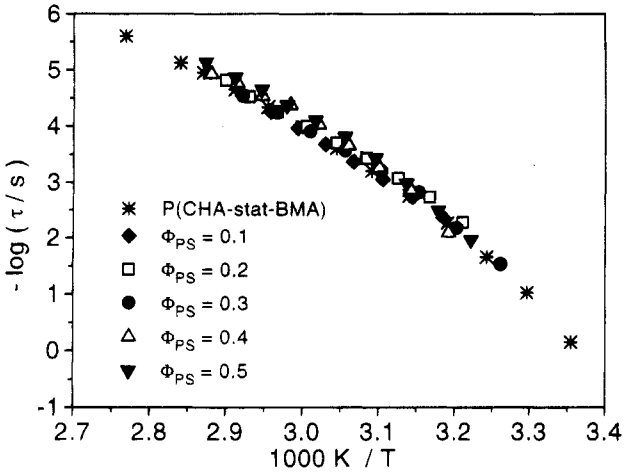

Figure 13. Temperature dependence of the relaxation time of P(CHA-*stat*-BMA) segments in the mixtures showing similar WLF behavior of the pure component.

pure polar component allows for a check of the self-consistency of the model. It is expected that the relaxation (HN) of P(CHA-*stat*-BMA) components should be independent of composition and show the same WLF parameters as the pure P(CHA-*stat*-BMA). Figure 13 shows an activation plot for the P(CHA-*stat*-BMA) in the mixtures. As expected, the temperature dependence of the relaxation time of the polar component does not change. The results obtained for PS/P(CHA-*stat*-BMA) confirm the assumption well up to 50% of polystyrene composition (Figure 13). A similar consistency of the model was shown for the system PVME/PS.[18]

Conclusions

The α-relaxation process provides access to a quantitative evaluation of the influence of concentration fluctuations on the molecular dynamics within the glass transition in polymer–polymer mixtures. The shape of the dielectric α-relaxation in the one-phase regime of PS/P(CHA-*stat*-BMA) mixtures was analyzed by using a model that assumes a Gaussian approximation for the concentration fluctuations and a Vogel–Fulcher–Tammann free volume scaling for the relaxation time that is dominated by P(CHA-*stat*-BMA). By fitting the measured loss curves $\epsilon''(\omega)$ to a model relaxation function for a mixture, the mean square concentration fluctuations $\langle(\delta\phi)^2\rangle$ at various temperatures above T_g were obtained. The $\langle(\delta\phi)^2\rangle$ values were combined with small-angle neutron scattering measurements for $S(q)$, and the size of the domains characterized by cooperative dynamics in the vicinity of the glass transition was calculated. The radius r of these domains in PS/P(CHA-*stat*-BMA) estimated for isotropic samples in the temperature range $T_g \le T \le T_g + 50$ K was between 6 and 10 nm for the composition range $\phi_{PS} = 0.2–0.5$. The radius r scales with temperature as $r \propto (T - T_0)^{-\nu}$ with $\nu \approx 2/3$ as predicted from the thermokinetic fluctuation approach of the glass transition. The half-widths $\delta_{1/2}$ log ω of the measured spectra show the temperature dependence $(\delta_{1/2} \log \omega)^{-1} \propto T - T_0$ and diverge at $T - T_g = C_2$. The half-widths of the loss curves as a function of $T - T_g$ show the same composition dependence as the $\langle(\delta\phi)^2\rangle$ values evaluated using the concentration fluctuation model when plotted against $T - T_g$.

Acknowledgment. The authors wish to thank Dr. A. Zetsche for kindly providing the software for the analysis using the concentration fluctuation model, Dr. W. Siol (Röhm GmbH, Darmstadt) for the statistical copolymer, and Th. Wagner (MPI für Polymerforschung) for the deuterated polystyrene. This work was supported by a grant from the Bundesministerium für Wirtschaft (AIF-Project No. 7695). G.K. thanks the German Academic Exchange Service (DAAD) and the Max Planck Institute for their financial support. V.A. thanks the European Community for a "Human Capital and Mobility" fellowship (No. ERBCHBICT930368).

References and Notes

(1) Bank, M.; Leffingwell, J.; Thies, C. *Macromolecules* **1971**, *4*, 43.
(2) Casper, R.; Morbitzer, L. *Angew. Makromol. Chem.* **1977**, *58/59*, 1.
(3) Cimmino; Karasz, F. E.; MacKnight, W. J. *J. Polym. Sci., B: Polym. Phys.* **1992**, *30*, 49.
(4) Chin, H. Y.; Zhang, C.; Wang, P.; Inglefield, P. J.; Jones, A. A.; Kambour, R. P.; Bendler, J. T.; White, D. M. *Macromolecules* **1992**, *25*, 3031.
(5) McCrum, N. G.; Read, B. E.; Williams, G. *Anelastic and Dielectric Effects in Polymeric Solids*; Wiley: London 1967.
(6) Miller, J. B.; McGrath, K. J.; Roland, C. M.; Trask, C. A.; Garroway, A. N. *Macromolecules* **1990**, *23*, 4543.
(7) Roland, C. M.; Ngai, K. L. *Macromolecules* **1991**, *24*, 2261.
(8) Brereton, M. G.; Fischer, E. W.; Fytas, G.; Murschall, U. *J. Chem. Phys.* **1987**, *86*, 5174. Murschall, U. Ph.D Dissertation, Mainz, 1986.
(9) Ishida, Y.; Yamamoto, M.; Takayanagi, M. *Kolloid Z.* **1960**, *124*, 168. Hedvig, P. *Dielectric Spectroscopy of Polymers*; Adam Hilger Ltd.: Bristol, 1977.
(10) Karasz, F. E.; MacKnight, W. J. In *Polymer Compatibility and Incompatibility*; Šole, K., Ed.; MMI Press Symposium Series; MMI Press: Midland, MI, 1982; Vol. 2.
(11) Zetsche, A.; Kremer, F.; Jung, H.; Schultze, H. *Polymer* **1990**, *31*, 1988. Zetsche, A. Ph.D Dissertation, Mainz, 1992.
(12) Katana, G.; Zetsche, A.; Kremer, F.; Fischer, E. W. *Polym. Prepr. (Am. Chem. Soc., Div. Polym. Chem.)* **1992**, *33*, 122. Katana, G.; Kremer, F.; Fischer, E. W.; Plaetschke, R. *Macromolecules* **1993**, *26*, 3075.
(13) Müller, G.; Stadler, R.; Schlick, S. *Macromolecules* **1994**, *27*, 1555.
(14) Shears, M. S.; Williams, G. *J. Chem. Soc., Faraday Trans.* **1973**, *69*, 608.
(15) Wetton, R. E.; MacKnight, W. J.; Fried, J. R.; Karasz, F. E. *Macromolecules* **1978**, *11*, 158.
(16) Alexandrovich, P. S.; Karasz, F. E.; MacKnight, W. J. *J. Macromol. Sci., Phys. (B)* **1980**, *17*, 501.
(17) Roland, C. M. *Macromolecules* **1987**, *20*, 2557.
(18) Fischer, E. W.; Zetsche, A. *Polym. Prepr. (Am. Chem. Soc., Div. Polym. Chem.)* **1992**, *33*, 78.
(19) Zetsche, A.; Fischer, E. W. *Acta Polym.* **1994**, *45*, 168.
(20) Ngai, K. L. *Comments Solid State Phys.* **1980**, *9*, 127. Ngai, K. L.; Rajagopal, A. K.; Teitler, S. J. *J. Chem. Phys.* **1988**, *88*, 5086.
(21) Roland, C. M.; Ngai, K. L. *Macromolecules* **1992**, *25*, 363.
(22) Havriliak, S.; Negami, S. *J. Polym. Sci., Part C* **1966**, *14*, 99.
(23) Colmenero, J.; Alegria, A.; Arbe, A.; Frick, B. *Phys. Rev. Lett.* **1992**, *69*, 478.
(24) Landau, L. D.; Lifschitz, E. M. *Lehrbuch der Theoretischen Physik, Statistische Physik*; Akademie-Verlag: Berlin, 1979; Teil 1, Band V.
(25) Hack, Th. Ph.D Thesis, in preparation 1995.
(26) de Gennes, P.-G. *Scaling Concepts in Polymer Physics*; Cornell University Press: Ithaca, NY, 1979.
(27) Pomposo, J. A.; Eguizabal, I.; Calahorra, E.; Cortázar, M. *Polymer* **1993**, *34*, 95.
(28) Donth, E. J. *Relaxation and Thermodynamics in Polymers*; Akademie-Verlag: Berlin, 1992.
(29) Fischer, E. W. *Mater. Res. Soc. Symp. Proc.* **1987**, *79*.
(30) Fischer, E. W. *Physica A* **1993**, *201*, 183.
(31) Ngai, K. L.; Roland, C. M.; O'Reilly, J. M.; Sedita, J. S. *Macromolecules* **1992**, *25*, 3906.
(32) Ruland, W. *Prog. Colloid Polym. Sci.* **1975**, *57*, 192.
(33) Adam, G.; Gibbs, J. H. *J. Chem. Phys.* **1965**, *43*, 139.
(34) Fischer, E. W.; Donth, E.; Steffen, W. *Phys. Rev. Lett.* **1992**, *68*, 2344.
(35) Matsuoka, S. *Proc. 18th North American Thermal Analysis Conf, San Diego, CA* **1989**, *1*, 126. Matsuoka, S.; Quan, X. *Macromolecules* **1991**, *24*, 2770.

MA946028A